Nicotinic acid–adenine dinucleotide phosphate activates the skeletal muscle ryanodine receptor

Martin HOHENEGGER[1], Josef SUKO, Regina GSCHEIDLINGER, Helmut DROBNY and Andreas ZIDAR

Department of Pharmacology, University of Vienna, Waehringerstrasse 13A, A-1090 Vienna, Austria

Calcium is a universal second messenger. The temporal and spatial information that is encoded in Ca^{2+}-transients drives processes as diverse as neurotransmitter secretion, axonal outgrowth, immune responses and muscle contraction. Ca^{2+}-release from intracellular Ca^{2+} stores can be triggered by diffusible second messengers like $Ins P_3$, cyclic ADP-ribose or nicotinic acid–adenine dinucleotide phosphate (NAADP). A target has not yet been identified for the latter messenger. In the present study we show that nanomolar concentrations of NAADP trigger Ca^{2+}-release from skeletal muscle sarcoplasmic reticulum. This was due to a direct action on the Ca^{2+}-release channel/ryanodine receptor type-1, since in single channel recordings, NAADP increased the open probability of the purified channel protein. The effects of NAADP on Ca^{2+}-release and open probability of the ryanodine receptor occurred over a similar concentration range ($EC_{50} \approx 30$ nM) and were specific because (i) they were blocked by Ruthenium Red and ryanodine, (ii) the precursor of NAADP, NADP, was ineffective at equimolar concentrations, (iii) NAADP did not affect the conductance and reversal potential of the ryanodine receptor. Finally, we also detected an ADP-ribosyl cyclase activity in the sarcoplasmic reticulum fraction of skeletal muscle. This enzyme was not only capable of synthesizing cyclic GDP-ribose but also NAADP, with an activity of 0.25 nmol/mg/min. Thus, we conclude that NAADP is generated in the vicinity of type 1 ryanodine receptor and leads to activation of this ion channel.

Key words: ADP-ribosyl cyclase, Ca^{2+}-release, sarcoplasmic reticulum.

INTRODUCTION

Ca^{2+} is an essential and universal intracellular messenger, and in most cells intracellular stores play a prominent role in initiating Ca^{2+} responses [1]. These intracellular stores are controlled by second messengers, which trigger Ca^{2+}-release by acting on ligand-gated ion channels. The currently known second messenger-controlled intracellular Ca^{2+}-channels comprise two families, the inositol 1,4,5-triphosphate ($Ins P_3$)-receptors and the ryanodine receptors. The members of the $Ins P_3$-receptor family are controlled by receptors that activate phospholipase C-isoforms and thereby generate $Ins P_3$ [2]. In contrast, the type 2 (cardiac isoform) and type 3 (brain isoform) ryanodine receptors are thought to function mainly as channels for Ca^{2+}-induced Ca^{2+}-release, and thus require the influx of trigger Ca^{2+} [3]. Opening of the skeletal muscle (type 1) ryanodine receptor is controlled by a direct interaction of the sarcolemmal L-type Ca^{2+}-channel, which acts as the voltage-sensor [4]. In addition, the activity of the ryanodine receptor/Ca^{2+}-release channel can be modulated by several endogenous (e.g. calmodulin, ATP) and exogenous ligands (ranging from the eponymic plant alkaloid ryanodine to suramin analogues) (reviewed in [5,6]).

In the past decade, two additional second messengers, cyclic ADP-ribose (cADP-ribose) and nicotinic acid–adenine dinucleotide phosphate (NAADP) were identified as controlling Ca^{2+}-release from intracellular stores. These new second messengers were originally found in sea urchin eggs but it is, at present, well appreciated that they are ubiquitously found in multi-cellular organisms as diverse as mammalian and plant cells (reviewed in [7–10]). Both nucleotides can be synthesized by the same class of enzymes, the ADP-ribosyl cyclase isoforms [11]. The mammalian family of ADP-ribosyl cyclases includes several poorly characterized enzymes; in contrast, the enzymology of CD38, a surface antigen of T-lymphocytes, is well characterized [11] and it is thus generally accepted that the enzyme is versatile enough to allow for the production of both cADP-ribose and NAADP by using NAD or NADP respectively [11].

Several recent studies have addressed the possibility that cADP-ribose and/or NAADP may release Ca^{2+} from intracellular stores by affecting ryanodine receptor isoforms either directly or indirectly [7]. This search was inspired by the observation that, in sea urchin eggs, an intracellular Ca^{2+}-release channel, which is apparently related to the mammalian ryanodine receptors, was stimulated by cADP-ribose (reviewed in [7,12]). However, the evidence obtained with vertebrate ryanodine receptor isoforms has been inconclusive. In Jurkat T-lymphocytes the Ca^{2+}-releasing actions of cADP-ribose is apparently accounted for by efflux from a ryanodine receptor-controlled pool [13]. However, in other mammalian tissues, in particular the myocardium, the concentrations of cADP-ribose required to trigger Ca^{2+}-release by ryanodine receptor activation were very high, i.e. in the micromolar range [14], and NAD, the precursor of cADP-ribose, or the breakdown product ADP ribose, were also effective [15].

In sea urchin eggs, NAADP-dependent Ca^{2+}-release displayed unique pharmacological properties, such that a direct action on the ryanodine receptor was considered improbable [12]. Nevertheless, when assayed directly, binding sites for NAADP in mammalian tissue were found to differ substantially from the binding sites identified in sea urchin eggs [16]. Recently, Chini

Abbreviations used: AMP-PNP, $\beta\gamma$-imidoadenosine 5′-triphosphate; cADP-ribose, cyclic ADP-ribose; cGDP-ribose, cyclic GDP-ribose; HSR, heavy sarcoplasmic reticulum; NAADP, nicotinic acid–adenine dinucleotide 2′-phosphate; 2′NADP, nicotinamide-adenine dinucleotide 2′-phosphate; 3′NADP, nicotinamide-adenine dinucleotide 3′-phosphate; NGD, nicotinamide-guanine dinucleotide.

[1] To whom correspondence should be addressed (e-mail: martin.hohenegger@univie.ac.at).

and co-workers described the synthesis of NAADP in a variety of mammalian tissues, including skeletal muscle [17]. While they have found coincidence of NAADP production and NAADP-induced Ca^{2+}-release in brain, heart, spleen and pancreas, the skeletal muscle was not investigated for a possible NAADP-sensitive Ca^{2+} pool.

We therefore examined the hypothesis that NAADP acted on the sarcoplasmic reticulum from skeletal muscle, which contains essentially a single form of the ryanodine receptors, namely the type 1 isoform. Our experiments show that NAADP, but not NADP or cADP-ribose, triggers Ca^{2+}-release from the sarcoplasmic reticulum at nanomolar concentrations and that the purified ryanodine receptor is a direct target of NAADP.

MATERIALS AND METHODS

Materials

NAD, nicotinamide-adenine dinucleotide 2′-phosphate (2′-NADP), nicotinamide-adenine dinucleotide 3′-phosphate (3′-NADP), NAADP, nicotinamide-guanine dinucleotide (NGD), cADP-ribose, cyclic GDP-ribose (cGDP-ribose), $\beta\gamma$-imidoadenosine 5′-triphosphate (AMP-PNP), Ruthenium Red, suramin, Ponceau S and leupeptin were purchased from Sigma (St. Louis, MI, U.S.A.). Alternatively, NAD, 2′-NADP and protease inhibitors were obtained from Roche Diagnostics (Vienna, Austria). [^{3}H]Ryanodine and the horseradish peroxidase-coupled anti-mouse antibody was from Amersham-Pharmacia (Freiburg, Germany) and lipids from Avanti Polar Lipids (Birmingham, LA, U.S.A.). The monoclonal antibody directed against the ryanodine receptor (clone 34C) was from Biomol (Hamburg, Germany) and the reagents for enhanced chemiluminescence detection were from Pierce (Rockford, IL, U.S.A.). All other reagents were of analytical grade.

Protein preparations

Heavy sarcoplasmic reticulum (HSR) membranes were prepared from rabbit white skeletal muscle as described previously [18,19]. For ryanodine receptor purification, the HSR membranes were solubilized in 1 % CHAPS (w/v) and the soluble fraction was used as a starting material to purify the ryanodine receptor by sucrose density centrifugation [20]. The proteoliposomes containing the purified ryanodine receptor were stored at −80 °C. The purity of the preparation was assessed by SDS/PAGE. Proteins were either visualized by staining with silver or, alternatively, transferred to nitrocellulose membranes and detected by Ponceau S. [^{3}H]Ryanodine binding was carried out as outlined previously [18].

ADP-ribosyl cyclase activity

ADP-ribosyl cyclase activity was determined by an assay that relies on the fluorescence increase caused by the formation of cGDP-ribose from NGD. The reaction was carried out in 250 μl buffer I, containing 20 mM Hepes/NaOH (pH 7.2), 0.5 mM $MgCl_2$, 0.45 mM $CaCl_2$, 0.5 mM EGTA, 15 mM NaCl and 125 mM KCl. HSR (50–70 μg) was allowed to equilibrate for 2 min before the reaction was started with 100 μM NGD. The fluorescence intensity was monitored at an excitation wavelength of 300 nm and an emission wavelength of 410 nm (using an F-4500 Hitachi fluorescence photometer). A calibration curve was generated with appropriate dilutions of cGDP-ribose to calculate the molar amount of cGDP-ribose formed by enzymatic action.

For the base-exchange reaction, the purified ADP-ribosyl cyclase (4 μg/ml) from *Aplysia* (Sigma) or HSR membranes (1 mg/ml) were incubated with 500 μM NADP, 1 mM nicotinic acid and buffer I, adjusted to a final pH of 5.0. The reaction mixture was incubated for 1 h at 37 °C in the dark and was immediately loaded onto an HPLC system for separation of the nucleotides.

HPLC analysis

Nucleotides from the base-exchange reaction were separated on an AG MP-1 column (4.6 mm × 26 mm, Bio-Rad) using a Hitachi HPLC system. The column was equilibrated in 100 % buffer A (water). The nucleotides were detected at 257 nm and eluted by a nonlinear gradient of trifluoroacetic acid at a flow rate of 1 ml/min: 0–2 min, 2 % B; 2–5 min, 4 % B; 5–9 min, 8 % B; 9–13 min, 16 % B; 13–20 min, 32 % B; 20–23 min, 100 % B (150 mM trifluoroacetic acid); 23–30 min, 0 % B. The specific activity of NAADP formation was determined from the area under curve of the NAADP peak and expressed as nmol/mg/min.

Release of [$^{45}Ca^{2+}$]

HSR (10 mg/ml) was passively loaded with 5 mM $^{45}CaCl_2$ (15–40000 c.p.m./nmol) in loading buffer, containing 50 mM Mops/Tris (pH 7.2), 120 mM KCl, 15 mM NaCl, 5 mM NaN_3 and a cocktail of protease inhibitors (0.5 μg/ml leupeptin, 1.4 μg/ml aprotinin, 1 μM pepstatin and 0.1 mM PMSF). After 24 h at 4 °C the HSR was diluted 100- or 200-fold in a nominally calcium-free loading buffer supplemented with 2 mM EGTA, 5 mM $MgCl_2$ and loaded onto a Bio-Logic rapid filtration system [21]. The HSR (50–100 μg) was kept on the filter (ME 26; Schleicher & Schuell, Dassel, Germany) and rinsed for the indicated times with release buffer, containing 50 mM Mops/Tris (pH 7.2), 120 mM KCl, 15 mM NaCl, 5 mM NaN_3 and the compounds indicated in the figure legends. In some experiments the pH of the buffer was set to 7.0 or 7.4. The free Ca^{2+} concentration was adjusted by the ratio of $CaCl_2$ and EGTA, using the algorithm and the stability constants of Schoenmaker and co-workers [22]. Time points longer than 10 s were determined manually using a conventional filtration device. The initial load was determined by extrapolation of the Ca^{2+}-release curve, with release buffer supplemented with 5 mM $MgCl_2$ and 20 μM Ruthenium Red at the start point of the release reaction. In order to determine the rapid Ca^{2+}-release rate the reaction was monitored over 30 s and the data points were fitted to a two-exponential equation [21].

Single channel recordings

The purified ryanodine receptor was fused into lipid bilayers formed by mixing phosphatidylserine and phosphatidylethanolamine in a 1:1 ratio (each dissolved in decane at 10 mg/ml). Single-channel recordings were carried out as described previously [19,20]. The *cis*-chamber and the *trans*-chamber were connected to the head-stage input of an EPC-9 amplifier (Heka Elektronik, Lambrecht, FRG); the *trans*-bath was held on virtual ground and Cs^+ was used as a charge carrier. The buffer composition in the *cis*-chamber was 10 mM Hepes/Tris (pH 7.4), 0.02–0.1 mM $CaCl_2$ and 480 mM CsCl, and in the *trans*-chamber, 10 mM Hepes/Tris (pH 7.4) and 50 mM CsCl. Purified Ca^{2+}-release channel/type 1 ryanodine receptor (1.5–2 μg) and other reagents were added to the *cis*-chamber. Recordings were filtered at 4 kHz through a low-pass Bessel filter, digitized at 40 kHz and subsequently stored on an Apple Macintosh computer. Single-channel events were analysed with TAC V2.5 software (Skalar Instruments, Seattle, WA). Mean open probability (P_o) of channels and

the corresponding lifetimes (τ) of the open and closed events were identified by a 50% threshold analysis. The holding potentials given in the figure legends were applied with reference to the *trans*-chamber. All experiments were carried out at 22–24 °C.

Miscellaneous procedures

Curve fitting was carried out using the standard Maquart-Levenberg algorithm provided by Sigma Plot (Jandl, San Rafael, CA). Statistical analysis was carried out by Students *t*-test and, for multiple comparisons, by ANOVA and Scheffe's *post hoc* test. Experiments were carried out at least three times and data are given as mean ± S.D., if not otherwise stated.

RESULTS

ADP-ribosyl cyclase activity in the sarcoplasmic reticulum

In order to search for ADP-ribosyl cyclase activity in the HSR, we made use of the fact that these enzymes accept NGD as substrate to form the fluorescent product cGDP-ribose (Figure 1A). Neither NGD nor GDP-ribose emit fluorescence at the wavelength pair employed. Hence, the experimental approach is suitable to continuously measure ADP-ribosyl cyclase activity, and to discriminate these enzymes from unrelated NADases [23].

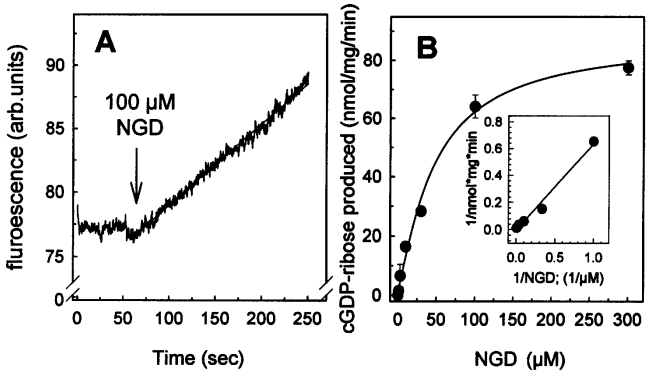

Figure 1 Characterization of ADP-ribosyl cyclase activity in the skeletal muscle HSR

(**A**) The formation of fluorescent cyclic GDP-ribose was monitored after the addition of 100 μM NGD, indicated by the arrow. The enzyme activity was calculated from linear regression which is overlaid on the increasing fluorescence trace after the addition of NGD. (**B**) The substrate saturation curve was generated under identical conditions. The inset depicts the Lineweaver–Burke transformation of the data.

During rabbit skeletal muscle HSR preparation, ADP-ribosyl cyclase activity was enriched approximately 12-fold compared with the starting material (post-nuclear homogenate; Table 1). During the first centrifugation step we lost 50% of the enzyme activity. The remaining functional enzyme was recovered throughout the consecutive purification steps. Two pools with ADP-ribosyl cyclase activity were identified. The first pool was in the 'cytosolic' fraction (supernatant of the first 30000 ***g*** pellet), where we recovered 39% of the enzyme activity, which most likely is due to a soluble ADP-ribosyl cyclase isoform. From the second pool, the 30000 ***g*** pellet, myosin and associated cytoskeletal proteins were extracted with 600 mM KCl. However, the enzyme activity resisted the high ionic strength, and was retained in the 100000 ***g*** pellet of the HSR. This observation suggests that the ADP-ribosyl cyclase of the HSR is an integral membrane protein, rather than a membrane-associated protein. The high-affinity [^{3}H]ryanodine-binding was carried out in parallel and enriched approximately 100-fold in the HSR compared with the starting material. The relatively high ADP-ribosyl cyclase activity in the post-nuclear homogenate, and possible sub-optimal assay conditions for the enzyme, may explain the discrepancy in the enrichment factors. Nevertheless, the ADP-ribosyl cyclase activity in the HSR was characterized by saturation isotherms and found to peak at 92.2 ± 10.3 nmol · mg^{-1} · min^{-1} (Figure 1B). NGD was utilized with a K_m of 53.3 ± 6.9 μM. This apparent affinity of the substrate is comparable to estimates of K_m observed with the isoforms found in T-lymphocytes (13 μM) [24] and *Aplysia* (119 μM) [25].

In addition to the cyclization reaction described by the formation of cGDP-ribose (Figure 1), the family of ADP-ribosyl cyclases have also been shown to catalyse a base-exchange reaction, to form NAADP from NADP and nicotinic acid [7,9,11,17]. In the present study, the reactants and products of the base-exchange reaction were separated on an anion-exchange column (Figure 2). The purified ADP-ribosyl cyclase from *Aplysia* was used as a standard and reached an activity of 1.2 μmol NAADP/mg/min (Figure 2C). Under identical ionic conditions, but using HSR as a source for ADP-ribosyl cyclase, an activity of 0.25 ± 0.05 nmol NAADP/mg/min (mean ± S.D., $n = 3$) was detectable (Figure 2D) and a symmetric NAADP peak eluted at 27.4 minutes (inset in Figure 2D).

NAADP-promoted Ca^{2+}-release from HSR vesicles

The principal function of the HSR in skeletal muscle is the storage and release of Ca^{2+} [1,6,26]. Because of the presence of an ADP-ribosyl cyclase in the HSR, and its ability to synthesize

Table 1 Enrichment of cGDP-ribose activity in HSR membranes

Three independent preparations of HSR were monitored for cGDP-formation under experimental conditions similar to those descriibed in Figure 1(A), using 100 μM NGD to initiate the reaction. The post-nuclear homogenate represents a precleared 4000 ***g*** supernatant which was termed the starting material. The first 30000 ***g*** supernatant corresponds to the 'cytosolic' fraction of the preparation. Data represent mean ± S.E.M. of six experiments. High-affinity [^{3}H]ryanodine binding was carried out for 2 h at 37 °C in the presence of 75 μg of protein, 20 nM [^{3}H]ryanodine, 20 mM HEPES (pH 7.4), 200 mM KCl, 10 mM NaCl and a free Ca^{2+} concentration of 20 μM. Data represent mean ± S.E.M. of three experiments done in duplicates; N.D. denotes not done.

	Protein (mg)	Specific activity (nmol · mg^{-1} · min^{-1})	Recovery (%)	[^{3}H]Ryanodine binding (pmol/mg)
Postnuclear homogenate	17375 ± 646	4.95 ± 0.56	100	0.014 ± 0.003
30000 ***g*** supernatant	16845 ± 909	2.0 ± 0.36	39.5	N.D.
30000 ***g*** pellet	495 ± 38	18.0 ± 0.96	10.5	0.37 ± 0.034
HSR	142 ± 15	60.1 ± 4.16	10.1	1.36 ± 0.14

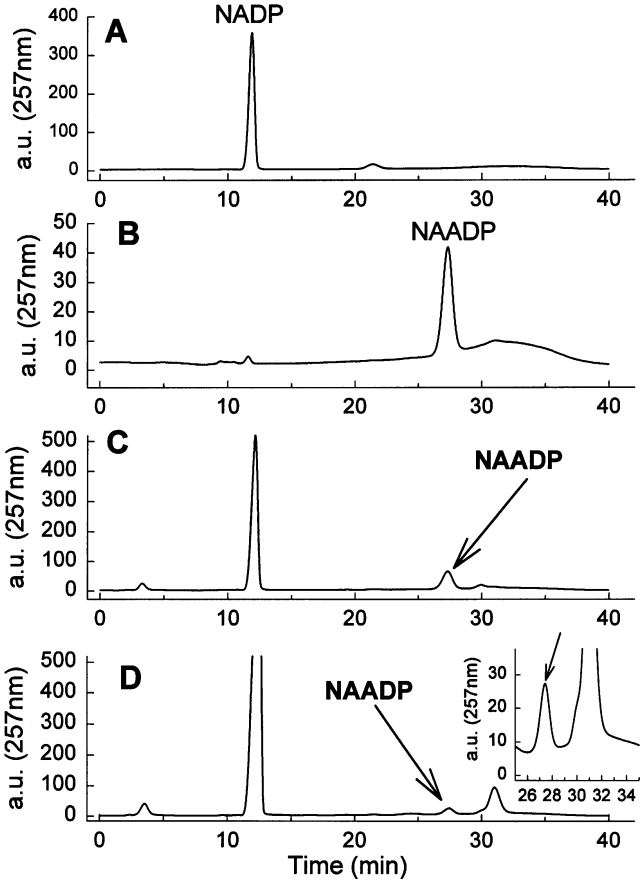

Figure 2 Synthesis of NAADP catalysed by an ADP-ribosyl cyclase in the skeletal muscle HSR

The HPLC analysis of the nucleotides was carried out with an anion-exchange column (AG MP-1) and detection at 257 nm. Commercially available standards for NADP [15 nmoles, (**A**)] and NAADP [2.5 nmoles, (**B**)] were used to calibrate the system. Aliquots of the base exchange reaction (20 μl) catalysed by the purified ADP-ribosyl cyclase [4 μg/ml, (**C**)] from *Aplysia* or HSR membranes [1 mg/ml, (**D**)] were analysed. The NAADP peak is indicated by an arrow and enlarged in the inset of (**D**). a.u., arbitrary units.

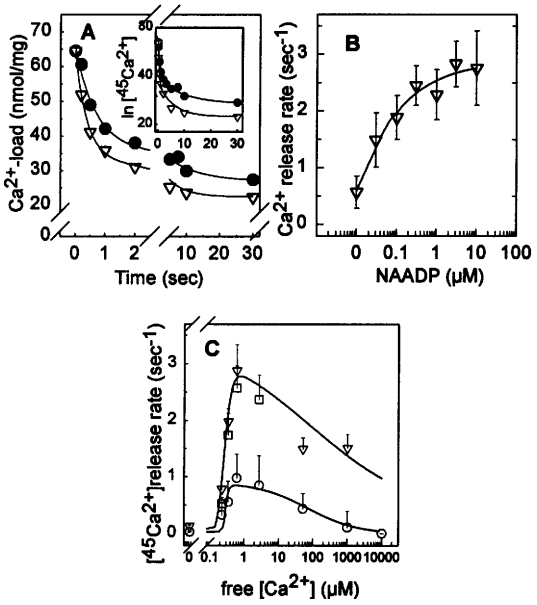

Figure 3 NAADP-induced [$^{45}Ca^{2+}$]-release from passively loaded HSR vesicles

(**A**) Passively loaded HSR vesicles (50–100 μg) were applied onto filters and Ca^{2+}-release was initiated by rinsing with release buffer (for composition see the Materials and methods section) containing 0.34 μM free Ca^{2+} in the absence (control, circles) and presence of 300 nM NAADP (triangles). At the time points indicated, the filter-bound radioactivity was determined. The lines were obtained by fitting the data by non-linear regression to an equation describing the sum of two exponential decays. The inset shows logarithmic transformation to illustrate the bi-exponential release kinetics and to show that NAADP only affects the rapid phase of Ca^{2+}-release. (**B**) Concentration-dependent acceleration by NAADP of Ca^{2+}-release from HSR. The release rates were determined at the indicated concentrations of NAADP as in (**A**). The calculated rate for the initial rapid release is plotted as a function of NAADP concentration. Data points represent the mean of three experiments which were carried out in duplicate; error bars indicate S.E.M. The solid line was drawn by fitting the data to a three-parameter logistic equation (Hill equation). (**C**) Ca^{2+}-induced Ca^{2+}-release from HSR vesicles in the absence (circles) and presence of 100 nM (triangles) or 300 nM NAADP (squares). Release rates were determined as in (**A**); the rate of rapid Ca^{2+}-release was plotted as a function of the free Ca^{2+} concentration. The zero point corresponds to determinations performed in Ca^{2+}-free Ca^{2+}-release buffer (containing 2 mM EGTA). The symbols represent the mean and error bars represent the S.E.M. ($n = 3$–7). The solid lines were fitted by fitting the data to the sum of two concentration-response curves.

NAADP, it was reasonable to postulate that the reaction product NAADP may affect Ca^{2+}-release. We therefore measured the rate of Ca^{2+}-efflux from passively loaded HSR vesicles by employing a rapid filtration device. Using this approach, incubation times in the sub-second range are possible and, thus, the complex kinetics of Ca^{2+}-induced Ca^{2+}-efflux can be resolved [21]. As can be seen from Figure 3(A), there are at least two phases of Ca^{2+}-release. Under basal conditions the initial rapid Ca^{2+}-release proceeded with a rate of $0.55 \pm 0.26\ s^{-1}$ ($n = 7$). These data were obtained from pooling three individual HSR preparations which may explain the mean variation. In the presence of 300 nM NAADP (triangles in Figure 3A), the initial efflux was significantly accelerated (rate $= 1.88 \pm 0.3\ s^{-1}$; $n = 4$, $P = 0.005$). It is evident from the logarithmic transformation depicted in the inset of Figure 3(A) that NAADP did not affect the second, slower component of Ca^{2+}-efflux. NAADP triggered the initial rapid Ca^{2+}-release (Figure 3B) with an EC_{50} of 32.8 ± 9.8 nM. This effect was specific, because at a concentration of 300 nM the precursor of NAADP, 2′-NADP, or the alternative reaction product, cADP-ribose, had no significant effect on rapid Ca^{2+}-release (control: $0.39 \pm 0.19\ s^{-1}$; 2′-NADP: $0.25 \pm 0.12\ s^{-1}$, cADP-ribose: $0.27 \pm 0.05\ s^{-1}$; mean $\pm$ S.E.M., $n = 3$; experimental conditions as in Figure 3A).

Ca^{2+}-release through the ryanodine receptors is subject to a bell-shaped regulation by Ca^{2+}, i.e. activation in the presence of submicromolar Ca^{2+} and inhibition at millimolar concentrations of Ca^{2+}. Several ryanodine receptor ligands, including caffeine [27], suramin [18,28] and the suramin analogue NF307 [18], sensitize the skeletal muscle ryanodine receptor to stimulation by Ca^{2+}. In order to prove this conjecture for NAADP, the free Ca^{2+} concentration in the release medium was varied from virtually zero to 10 mM (Figure 3C). NAADP accelerated the rate of Ca^{2+}-release over the entire Ca^{2+} concentration range but a shift in the EC_{50} of activating Ca^{2+} was not observed (control: 0.28 ± 0.06 μM; 300 nM NAADP 0.27 ± 0.03 μM). Interestingly, in the presence of 300 nM NAADP, millimolar concentrations of Ca^{2+} were less effective in preventing activation of the ryanodine receptor. This effect was also observed previously for suramin, a ryanodine receptor-channel opener [28]. In the present study, the pH of the release medium was also varied from 7.0 to 7.4. However, there was no significant difference in Ca^{2+}-release rates

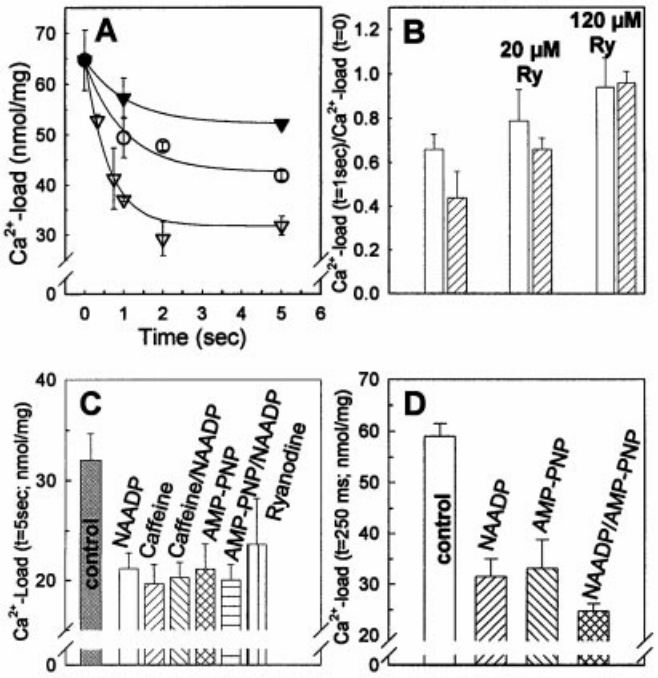

Figure 4 Inhibition of the NAADP induced Ca^{2+}-release by Ruthenium Red and ryanodine

(**A**) Ca^{2+}-release from passively loaded HSR vesicles was induced by release buffer containing 0.34 μM free Ca^{2+} (open circles), plus 300 nM NAADP (open triangles) or 300 nM NAADP and 2 μM Ruthenium Red (black triangles); reaction conditions were otherwise similar to those in Figure 1(A). (**B**) Ca^{2+}-release from passively loaded HSR was triggered for 1 s by release medium, containing 0.34 μM free Ca^{2+} in the absence (white bar) or presence of 300 nM NAADP (hatched bars). Aliquots of the passively loaded HSR had been pre-incubated with 20 μM or 120 μM ryanodine for 2 h (indicated as 20 μM Ry and 120 μM Ry respectively). The amount of radioactivity retained in the vesicles after 1 s was related to the amount of radioactivity present originally (i.e. at time = 0). The latter was 65.3 $\pm$ 7 nmol/mg. (**C**) Ca^{2+}-release was triggered from passively loaded HSR vesicles for 5 s in release buffer containing 0.34 μM free Ca^{2+} alone (control), 300 nM NAADP, 10 mM caffeine, 0.4 mM AMP-PNP, 10 nM ryanodine or NAADP in combination with caffeine and AMP-PNP at given concentrations. The amount of vesicle-trapped [$^{45}Ca^{2+}$] was determined after 5 s. The Ca^{2+} level at time = 0 was 73.2 $\pm$ 2.5 nmol/mg. Data represent mean $\pm$ S.D. of three experiments carried out in quadruplicate. (**D**) Ca^{2+}-release (69.8 $\pm$ 2.6 nmol/mg) from passively loaded HSR was measured at 0.7 μM free Ca^{2+} under conditions given in the legend to Figure 1A. The remaining radioactivity was measured after 250 ms in the absence (control) or presence of 300 nM NAADP (NAADP), 0.4 mM AMP-PNP (AMP-PNP) or 300 nM NAADP plus 0.4 mM AMP-PNP (NAADP/AMP-PNP). Single factor analysis of variance (ANOVA) and subsequent Scheffé *post hoc* comparison of the data identified significant difference between the control and NAADP, AMP-PNP, and NAADP/AMP-PNP-induced open probabilities ($P < 0.0001$) and AMP-PNP and NAADP/AMP-PNP-induced open probabilities ($P < 0.05$). Data represent mean $\pm$ S.D. of three experiments carried out in quadruplicate.

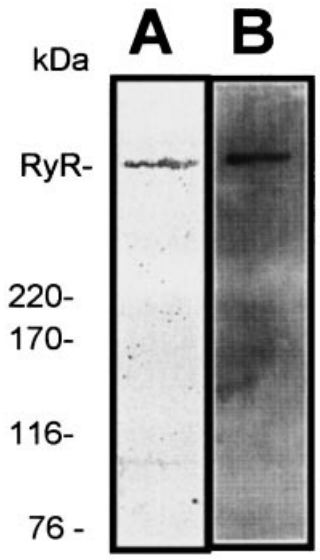

Figure 5 Documentation of the homogeneity of the purified ryanodine receptor

The purified ryanodine receptor (2.5 μg/lane) was loaded onto a 7% SDS/PAGE, transferred onto a nitrocellulose membrane and stained with Ponceau S (lane A). A single band was confirmed to be the ryanodine receptor using a specific antibody (1:2000 dilution, lane B). RyR indicates the ryanodine receptor band and the numbers indicate the molecular mass standards, myosin (220 kDa), α_2-macroglobulin (170 kDa), β-galactosidase (116 kDa), transferrin (76 kDa).

with 100 or 300 nM NAADP at pH 7.0, 7.2 or 7.4 (results not shown).

We have verified that NAADP-triggered Ca^{2+}-release occurred through the ryanodine receptor/Ca^{2+} release-channel by the following pharmacological criteria: (i) Ruthenium Red is a blocker of the ryanodine receptor at concentrations in the low micromolar range [29]. Accordingly, the NAADP-induced, rapid Ca^{2+}-release was abrogated by 2 μM Ruthenium Red (Figure 4A). (ii) The dual actions of the plant alkaloid ryanodine, activation at low nanomolar concentrations and inhibition at micromolar concentrations, were used to induce Ca^{2+}-release and to block NAADP-induced Ca^{2+}-release (Figures 4B and 4C). However, the association of ryanodine to the inhibitory binding site proceeds very slowly. Hence, it is difficult to achieve a complete inhibition within the time scale used in rapid filtration experiments. In order to overcome this experimental limitation we exploited the very slow dissociation of ryanodine from the low affinity binding site [28]. Preincubation with 20 or 120 μM ryanodine prior to the Ca^{2+}-release experiments prevented Ca^{2+}- and NAADP-induced Ca^{2+}-release in a dose-dependent fashion (Figure 4B). (iii) If the Ca^{2+}-releasing effect of NAADP is mediated through its action on the ryanodine receptor, the combination of NAADP and other ryanodine receptor-channel openers should be non-additive when assayed at a time point where the NAADP-stimulated rapid release approaches completion, i.e. after 5 s (cf. Figure 3A). It is evident from Figure 4(C) that 5 s after stimulation, the amounts of vesicle-trapped [$^{45}Ca^{2+}$] were comparable, regardless of whether each individual compound (caffeine or AMP-PNP) was added alone or in combination with NAADP. Finally, the effect of NAADP was similar in magnitude to the effect of 10 nM ryanodine, i.e. a concentration that activates the ryanodine receptor. Based on these observations, we conclude that NAADP releases Ca^{2+} from the same vesicle population, and hence from the same store, as ryanodine receptor channel-openers. The fact that NAADP and AMP-PNP were not additive in releasing Ca^{2+} from HSR does not prove that NAADP is ineffective in the presence of AMP-PNP. It is possible that NAADP accelerates only the initial Ca^{2+}-release rate, which should be detectable in the initial time points. As shown in Figure 4(D), within 250 ms the amount of intravesicular Ca^{2+} is significantly diminished in the presence of 300 nM NAADP or 0.4 mM AMP-PNP (multiple comparison using ANOVA and *post hoc* Scheffe test; $P < 0.0001$). Furthermore, using a saturating concentration of 300 nM NAADP, the Ca^{2+}-release was significantly augmented by the co-administration of 0.4 mM AMP-PNP compared with AMP-PNP

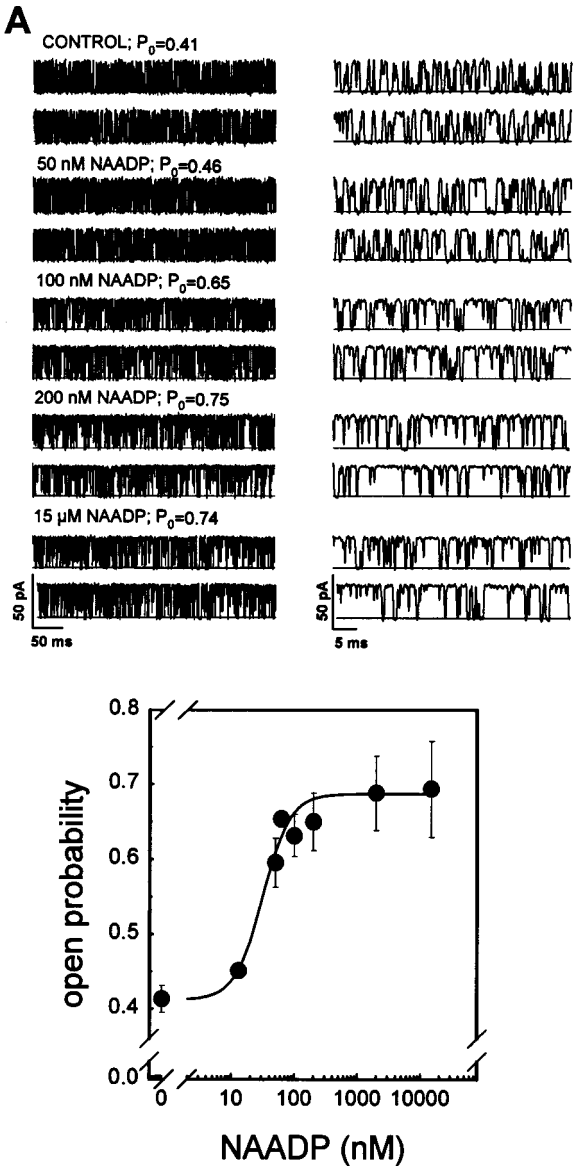

Figure 6 Activation by NAADP of a single purified skeletal muscle Ca^{2+}-release channel

(**A**) Single-channel currents shown as upward deflections were recorded at +20 mV holding potential with 480 mM/50 mM CsCl (*cis*/*trans*) and 20 μM Ca^{2+} (*cis*). NAADP was added sequentially to the *cis* side and recordings were made 5 min thereafter. Control and test recordings are from the same channel. The baselines (solid lines) indicate the closed state of the channel. The left panel shows 400 ms recordings and the right panel the first 40 ms of each recording. (**B**) Concentration-dependent stimulation of the open probability (P_o) of the purified ryanodine receptor by NAADP. The concentration-response curve was obtained by determining P_o as in (**A**). Data represent mean ± S.E.M., $n = 3$–19.

alone ($P < 0.05$). Taken together, these data provide evidence that even in the presence of an adenine nucleotide, NAADP preserves its Ca^{2+}-mobilizing ability.

Direct activation of the type 1 ryanodine receptor channel by NAADP

In order to confirm that the NAADP-induced Ca^{2+}-release arises from a direct interaction with the ryanodine receptor, single-channel recordings were carried out with the purified ryanodine receptor. A protein stain and the corresponding immunoblot analysis of a representative purified ryanodine receptor preparation is shown in Figure 5. After inserting the channel protein in artificial lipid bilayers, NAADP increased the open probability in a concentration-dependent manner (Figure 6, Table 2). An EC_{50} of 31.2 ± 6.9 nM was estimated from the concentration-response curve (Figure 6B), which is similar to the estimate obtained in Ca^{2+}-release experiments. NAADP was only effective when added from the cytosolic (*cis*) side of the channel. The single-channel current amplitude was not altered by the addition of increasing concentrations of NAADP (Table 2). NAADP-mediated activation of the ryanodine receptor (exemplified for 100 nM NAADP) increased the mean open duration (T_o) and shortened the mean closed duration (T_c) significantly (Table 3). In line with these findings, the open time constant (τ_{o1}) was significantly increased, whilst the close time constant (τ_{c1}) was significantly reduced compared with control (Table 3). Thus, the increase in the open probability by the application of NAADP was, at least in part, due to longer open states of the channel protein. For comparison, an electrophysiological analysis was carried out in parallel with the universal ryanodine receptor agonist suramin [28,30]. At saturating suramin concentrations (900 μM), we determined an open probability of 0.82 ± 0.03, a value similar to previous reports [20,28]. Although the open probabilities after addition of suramin or of NAADP are reasonably similar in magnitude, the compounds achieve this increase in open probability by distinct actions: in the presence of suramin, the channel is shifted into a state with long open times (τ_{o2} and τ_{o3} in Table 3). In contrast, NAADP does not alter the distribution of open states but, as stated above, prolongs τ_{o1} (Table 3). In 4 out of 19 single channel recording experiments, an increase in the open probability on sequential addition of 50–200 nM NAADP was followed by a decline of the open probability on further addition of NAADP. The reason for this reduction in the open probability is unknown. In two out of these four experiments, the Ca^{2+}-release channel could be reactivated by 15–30 μM NAADP. From these experiments it is concluded that, in contrast to the observations in the sea urchin eggs and pancreatic acinar cells, the purified skeletal muscle ryanodine receptor is not desensitized upon addition of nanomolar or micromolar concentrations of NAADP [7,12].

Table 2 Concentration-dependent effect of NAADP in single-channel recordings of the purified skeletal muscle ryanodine receptor

Single-channel currents of the purified ryanodine receptor were recorded at a holding potential of 20 mV under conditions given in the legend to Figure 3. Open probabilities and amplitudes are shown as means ± S.E.M. and the number of experiments is given in parentheses. *Single-factor analysis of variance (ANOVA) and subsequent Scheffé *post hoc* comparison of the data identified significant difference between controls and NAADP-induced open probabilities as indicated ($P < 0.0005$).

	Open probability	Amplitude (pA)
Control	0.41 ± 0.01 (19)	30.5 ± 0.5 (19)
50 nM NAADP	0.59 ± 0.03* (17)	32.2 ± 1.1 (17)
100 nM NAADP	0.63 ± 0.03* (13)	31.8 ± 0.9 (13)
15 μM NAADP	0.69 ± 0.06* (7)	29.3 ± 0.7 (7)

The ryanodine receptor displays a linear current-voltage relationship at holding potentials ranging from −20 mV to 60 mV (data not shown). Unitary currents were measured under conditions similar to those given in Figure 6, in the absence and presence of 2 μM NAADP. The calculated reversal potentials were virtually identical (−48.9 mV in the absence and −49.8 mV in the presence of 2 μM NAADP). Similarly, the conductance (estimated from the slope of the regression line) was not affected

Table 3 Electrophysiological parameters of single-channel recordings of the ryanodine receptor stimulated by NAADP or suramin

Single-channel currents of the purified ryanodine receptor were recorded at a holding potential of 20 mV and conditions given in the legend to Figure 3. Data represent means ± S.E.M. P_o designates the open probability, T_o the mean open duration and T_c the mean close duration. The percentage of area corresponding to individual open (τ_o) and closed (τ_c) time constants was calculated from lifetime histograms and is given in parentheses. Significant differences were identified by Student's *t*-test and are indicated by asterisks: *($P < 0.0005$), **($P < 0.000\,05$).

	Control for NAADP ($n = 13$)	100 nM NAADP ($n = 13$)	Control for suramin ($n = 8$)	0.9 mM suramin ($n = 8$)
P_o	0.42 ± 0.03	0.63 ± 0.03**	0.47 ± 0.04	0.82 ± 0.03**
Amplitude (pA)	30.9 ± 0.54	31.8 ± 0.9	30.3 ± 0.54	30.4 ± 1.3
T_o (ms)	0.38 ± 0.02	0.57 ± 0.04**	0.4 ± 0.03	1.2 ± 0.24**
T_c (ms)	0.51 ± 0.03	0.36 ± 0.03*	0.45 ± 0.05	0.27 ± 0.03*
τ_{o1} (ms)	0.24 ± 0.01 (79 ± 2%)	0.37 ± 0.03* (80 ± 3%)	0.3 ± 0.02 (80 ± 3%)	0.35 ± 0.07 (41 ± 4%)
τ_{o2} (ms)	0.82 ± 0.19 (21 ± 2%)	1.11 ± 0.09 (20 ± 3%)	0.7 ± 0.06 (17 ± 3%)	1.4 ± 0.24* (47 ± 3%)
τ_{o3} (ms)	–	–	–	5.5 ± 1.05 (10 ± 1%)
τ_{c1} (ms)	0.37 ± 0.02 (80 ± 3%)	0.24 ± 0.02** (92 ± 3%)	0.31 ± 0.01 (82 ± 11%)	0.14 ± 0.02* (78 ± 4%)
τ_{c2} (ms)	1.32 ± 0.14 (20 ± 3%)	1.30 ± 0.36 (9 ± 4%)	1.58 ± 0.63 (23 ± 14%)	0.48 ± 0.1* (20 ± 4%)

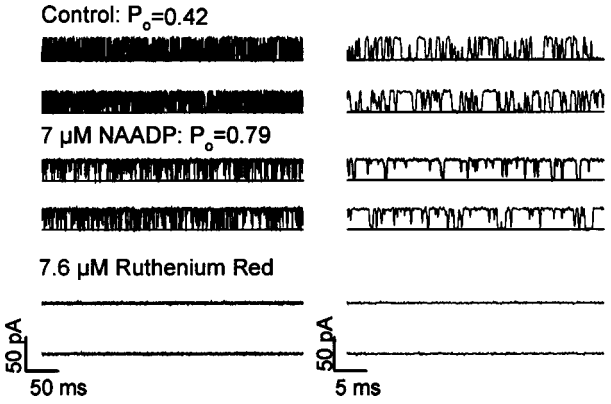

Figure 7 Inhibition by Ruthenium Red of NAADP-activated single-channel currents through the purified ryanodine receptor

Single-channel currents, shown as upward deflections, were recorded at 20 mV holding potential with 480 mM/50 mM CsCl (*cis*/*trans*). The baselines corresponding to the closed state of the channel are indicated by solid lines. The compounds were added sequentially to the *cis* side, 100 μM $CaCl_2$ (control), 7 μM NAADP and 7.6 μM Ruthenium Red. The left traces cover 400 ms recordings, and out of that 40 ms are shown on the right side. Calibration bars represent 50 pA and 50 ms or 5 ms. Data are from a representative experiment; two additional experiments gave similar results.

by NAADP (control: 538 pS; 2 μM NAADP: 526 pS). The high conductance of approximately 530 pS is typical for recordings performed with Cs^+ as the charge carrier [6] and essentially identical to our previous observations [20].

We confirmed that NAADP specifically activated the ryanodine receptor by the following experiments. The ryanodine-receptor blocker, Ruthenium Red, completely abrogated the currents elicited by a high (saturating) concentration of NAADP and the channel was locked in the closed state (Figure 7). Finally, we also tested the enzymatic precursor of NAADP, 2′-NADP, which did not activate the purified ryanodine receptor in single-channel recordings. At 300 nM, a concentration at which NAADP fully activated the channel (see Figure 6B and Table 2), 2′-NADP did not have any appreciable effect (control: $P_o = 0.402 \pm 0.049$, $n = 8$; 300 nM 2′-NADP: $P_o = 0.458 \pm 0.076$, $n = 8$). 3′-NADP was also investigated in order to evaluate the importance of the position of the ribosyl phosphate group; this analogue was also not effective in stimulating the Ca^{2+}-release channel (control: $P_o = 0.44 \pm 0.06$; $n = 4$; 300 nM 3′-NADP: $P_o = 0.45 \pm 0.07$, $n = 4$).

DISCUSSION

In the present work, we provide compelling evidence for a direct action of NAADP on the skeletal muscle ryanodine receptor type 1. We show that NAADP triggered rapid Ca^{2+}-release from skeletal muscle sarcoplasmic reticulum and that this release was dependent on the type 1 ryanodine receptor because it was blocked by Ruthenium Red and micromolar concentrations of ryanodine. The Ca^{2+} pool controlled by NAADP was similar in size to that controlled by typical ryanodine receptor channel openers (caffeine, AMP-PNP and, at nanomolar concentrations, ryanodine). The ability of NAADP to release Ca^{2+} from HSR vesicles can be fully accounted for by an NAADP-dependent direct activation of the ryanodine receptor. Both Ca^{2+}-release from HSR and single channel currents of the purified ryanodine receptor were activated by NAADP, with essentially identical EC_{50} values of ≈ 30 nM. Finally, NAADP-activated single-channel currents did not differ in conductance and reversal potential from the Ca^{2+}-activated currents, and Ruthenium Red completely abrogated NAADP-activated single channel currents. These two sets of observations rule out the possibility that the electrophysiological effects of NAADP were due to its action on a different channel protein that contaminated the purified ryanodine receptor preparation. Although unlikely, it cannot be ruled out that an accessory protein tightly associated with the ryanodine receptor is mediating the NAADP-induced activation.

The action of NAADP on both Ca^{2+}-release and single-channel currents was specific because it was mimicked neither by the precursor substrate 2′-NADP nor by the alternative product of the enzymatic reaction, cADP-ribose. Similarly, 3′-NADP, a structural analogue of 2′-NADP, was ineffective. This indicates that it is not the relative position of the PO_4-moiety but the nicotinic acid-moiety that is important for biological activity.

NAADP displays a high apparent affinity for the type 1 ryanodine receptor; the EC_{50} (≈ 30 nM) is comparable to that described for Ca^{2+}-release in some mammalian cells, e.g. pancreatic acinar cells [31] and Jurkat T-lymphocytes [32], as well as sea urchin eggs [33,34] and plants [35]. Recently, the type 2 ryanodine receptor from dogs, which represents the cardiac isoform, was found to respond to NAADP in single-channel recordings at concentrations exceeding 1 μM [36]. However, it is not clear whether the effect of NAADP reflects a direct action on the ryanodine receptor, because experiments were evaluated on microsomal membrane preparations rather than on the purified ryanodine receptor. Bak and co-workers [37] observed that NAADP-triggered Ca^{2+}-release from rabbit cardiac microsomes was blocked neither by inhibitors of the $InsP_3$-receptor nor by

the specific ryanodine receptor blockers, ryanodine (100 μM) and Ruthenium Red (5 μM). Our experiments, however, show that, at comparable concentrations and under comparable experimental conditions, these compounds fully blocked Ca^{2+}-release from skeletal muscle HSR vesicles.

In part, our observations are controversial in the light of results recently published by Copello and co-workers [38]. NAADP and cADP-ribose had no effect on the Ca^{2+}-uptake, nor could it effect open probability in single-channel recordings of sarcoplasmic reticulum membranes from rabbit skeletal muscle. We have not investigated Ca^{2+}-uptake into the HSR in the presence of the Ca^{2+}-releasing agents NAADP or cADP-ribose because conclusions on a possible Ca^{2+}-release mechanism may only be drawn indirectly and therefore are not conclusive. However, we could confirm the finding that cADP-ribose is not able to induce Ca^{2+}-release from HSR, but in contrast NAADP unequivocally triggers Ca^{2+}-release (Figures 3 and 4). The difference in the electrophysiological results of the present study and the investigation mentioned above are not clear. However, our experimental conditions differ markedly from those reported by Copello and co-workers [38] in the following ways: (i) we studied purified type 1 ryanodine receptor in electrophysiological experiments in contrast with sarcoplasmic reticulum fractions; (ii) Cs^{+} was used as a permeant ion instead of Ca^{2+}; (iii) in all electrophysiological experiments we have only analysed NAADP effects on single-channel recordings of the purified ryanodine receptor whereas Copello and co-workers have allowed multiple channel fusions, which may have occluded detection of a direct activation of a single ryanodine receptor by NAADP; and (iv) under these conditions the ryanodine receptors exhibit a fast heterogeneity in gating, ranging from a very low open probability of less than 0.1 to greater than 0.8 (under identical conditions of 100 μM free Ca^{2+}). Moreover, calmodulin, which is known to inhibit the skeletal muscle ryanodine receptor in the presence of micromolar concentrations of Ca^{2+} [6], had only a modest or, in some cases, no effect on the open probability [38].

Previously, ADP-ribosyl cyclase activity was observed in membrane fractions from cardiac ventricle [17,39] and, more recently, from skeletal muscle homogenates [17,40]. We confirmed that ADP-ribosyl cyclase activity is present in skeletal muscle. Throughout the preparation of the HSR, the membranes were exposed to 600 mM KCl, a high ionic strength that could not release ADP-ribosyl cyclase activity from the HSR. This is indicative for a tightly associated membrane protein or possibly an integral membrane protein. More importantly, we observed that ADP-ribosyl cyclase activity was substantially enriched in HSR vesicles, such that the specific activity was substantially higher than that determined in an unfractionated membrane preparations from skeletal muscle. In a recent report, the enzymatic formation of NAADP was directly measured in 100 000 ***g*** membranes from rat skeletal muscle and accounted to be 0.07 nmol/mg/min [17]. However, the ability of NAADP to release Ca^{2+} in this tissue was not further investigated. We could confirm synthesis of NAADP in skeletal muscle membranes. With an activity of 0.25 nmol/mg/min, the ADP-ribosyl cyclase seems to be enriched in HSR membranes compared with the membranes used by Chini and co-workers [17]. Thus it is safe to conclude that in skeletal muscle the second messenger NAADP can be generated in the vicinity of its target, the type 1 ryanodine receptor. The physiological role of the NAADP induced Ca^{2+}-release and ryanodine receptor activation is not clear at the moment.

We thank Anton Karel and Gertrude Hellmann for technical assistance and Michael Freissmuth and Lukas Weigl for helpful discussions. This work was supported by the Fonds zur Foerderung der wissenschaftlichen Forschung (P-14940 to M.H.), Anton Dreher Gedächtnisschenkung (to M.H.), Hochschuljubiläumsstiftung der Stadt Wien (to M.H.) and Hans und Bianca Moser-Stiftung (to A.Z.).

REFERENCES

1 Berridge, M. J. (1993) Cell signalling. A tale of two messengers. Nature (London) **361**, 315–325
2 Berridge, M. J., Bootman, M. D. and Lipp, P. (1998) Calcium: a life and death signal. Nature (London) **395**, 645–648
3 Sorrentino, V. and Volpe, P. (1993) Ryanodine receptors: how many, where and why? Trends Phamacol. Sci. **14**, 98–103
4 Protasi, F., Takekura, H., Wang, Y., Chen, S. R., Meissner, G., Allen, P. D. and Franzini-Armstrong, C. (2000) RYR1 and RYR3 have different roles in the assembly of calcium release units of skeletal muscle. Biophys. J. **79**, 2494–2508
5 Zucchi, R. and Ronca-Testoni, S. (1997) The sarcoplasmic reticulum Ca^{2+} channel/ryanodine receptor: modulation by endogenous effectors, drugs and disease states. Pharmacol. Rev. **49**, 1–51
6 Meissner, G. (1994) Ryanodine receptor/Ca^{2+} release channels and their regulation by endogenous effectors. Annu. Rev. Physiol. **56**, 485–508
7 Lee, H. C. (2001) Physiological functions of cyclic ADP-ribose and NAADP as calcium messengers. Ann. Rev. Pharmacol. Toxicol. **41**, 317–345
8 Guse, A. H. (1999) Cyclic ADP-ribose: a novel Ca^{2+}-mobilising second messenger. Cell. Signalling **11**, 309–316
9 Lee, H. C. (1997) Mechanisms of calcium signaling by cyclic ADP-ribose and NAADP. Physiol. Rev. **77**, 1133–1164
10 Genazzani, A. A. and Galione, A. (1997) A Ca^{2+} release mechanism gated by the novel pyridine nucleotide, NAADP. Trends Pharmacol. Sci. **18**, 108–110
11 Lee, H. C. (2000) Enzymatic functions and structures of CD38 and homologs. Chem. Immunol. **75**, 39–59
12 Patel, S., Churchill, G. C. and Galione, A. (2001) Coordination of Ca2+ signalling by NAADP. Trends Biochem. Sci. **26**, 482–489
13 Guse, A. H., Da Silva, C. P., Berg, I., Skapentko, A. L., Weber, K., Heyer, P., Hohenegger, M., Ashamu, G. A., Schulz-Koops, H., Potter, B. V. L. and Mayr, G. W. (1999) Regulation of calcium signalling in T lymphocytes by the second messenger cyclic ADP-ribose. Nature (London) **398**, 70–73
14 Meszaros, L. G., Bak, J. and Chu, A. (1993) Cyclic ADP-ribose as an endogenous regulator of the non-skeletal type ryanodine receptor Ca^{2+} channel. Nature (London) **364**, 76–79
15 Sitsapesan, R. and Williams, A. J. (1995) The gating of the sheep skeletal sarcoplasmic reticulum Ca($^{2+}$)-release channel is regulated by luminal Ca^{2+}. Am. J. Physiol. **268**, C1235–C1240
16 Patel, S., Churchill, G. C., Sharp, T. and Galione, A. (2000) Widespread distribution of binding sites for the novel Ca^{2+}-mobilizing messenger, nicotinic acid adenine dinucleotide phosphate, in the brain. J. Biol. Chem. **275**, 36495–36497
17 Chini, E. N., Chini, C. C. S., Kato, I., Takasawa, S. and Okamoto, H. (2002) CD38 is the major enzyme responsible for synthesis of nicotinic acid-adenine dinucleotide phosphate in mammalian tissues. Biochem. J. **362**, 125–130
18 Klinger, M., Freissmuth, M., Nickel, P., Stäbler-Schwarzbart, M., Kassack, M., Suko, J. and Hohenegger, M. (1999) Suramin and suramin analogs activate skeletal muscle ryanodine receptor via a calmodulin binding site. Mol. Pharmacol. **55**, 462–472
19 Suko, J. and Hellmann, G. (1998) Modification of sulfhydryls of the skeletal muscle calcium release channel by organic mercurial compounds alters Ca^{2+} affinity of regulatory Ca^{2+} sites in single channel recordings and [3H]ryanodine binding. Biochim. Biophys. Acta **1404**, 435–450
20 Suko, J., Hellman, G. and Drobny, H. (2001) Short- and long-term functional alterations of the skeletal muscle calcium release channel (ryanodine receptor) by suramin: apparent dissociation of single channel current recording and [3H]ryanodine binding. Mol. Pharmacol. **59**, 543–556
21 Wyskovsky, W., Hohenegger, M., Plank, B., Hellmann, G., Klein, S. and Suko, J. (1990) Activation and inhibition of the calcium-release channel of isolated skeletal muscle heavy sarcoplasmic reticulum. Models of the calcium-release channel. Eur. J. Biochem. **194**, 549–559
22 Schoenmakers, J. M., Visser, G. J., Flick, G. and Theuvene, A. P. R. (1992) Chelator: An improved method of computing metal ion concentrations in physiological solutions. BioTechniques **12**, 870–879
23 Graeff, R. M., Walseth, T. F., Fryxell, K., Branton, W. D. and Lee, H. C. (1994) Enzymatic synthesis and characterizations of cyclic GDP-ribose. A procedure for distinguishing enzymes with ADP-ribosyl cyclase activity. J. Biol. Chem. **269**, 30260–30267
24 da Silva, C. P., Schweitzer, K., Heyer, P., Malavasi, F., Mayr, G. W. and Guse, A. H. (1998) Ectocellular CD38-catalyzed synthesis and intracellular Ca^{2+}-signalling activity of cyclic ADP-ribose in T-lymphocytes are not functionally related. FEBS Lett. **439**, 291–296

25 Munshi, C., Thiel, D. J., Mathews, I. I., Aarhus, R., Walseth, T. F. and Lee, H. C. (1999) Characterization of the active site of ADP-ribosyl cyclase. J. Biol. Chem. **274**, 30770–30777
26 Coronado, R., Morrissette, J., Sukhareva, M. and Vaughan, D. M. (1994) Structure and function of ryanodine receptors. Am. J. Physiol. **266**, C1485–C1504
27 Rousseau, E., LaDine, J., Liu, Q. and Meissner, G. (1988) Activation of the Ca^{2+} release channel of skeletal muscle sarcoplasmic reticulum by caffeine and related compounds. Arch. Biochem. Biophys. **267**, 75–86
28 Hohenegger, M., Matyash, M., Poussu, K., Herrmann-Frank, A., Sarközi, S., Lehmann-Horn, F. and Freissmuth, M. (1996) Activation of the skeletal muscle ryanodine receptor by suramin and suramin analogs. Mol. Pharmacol. **50**, 1443–1453
29 Smith, J. S., Coronado, R. and Meissner, G. (1985) Sarcoplasmic reticulum contains adenine nucleotide-activated calcium channels. Nature (London) **316**, 446–449
30 Hohenegger, M., Berg, I., Weigl, L., Mayr, G. W., Potter, B. V. and Guse, A. H. (1999) Pharmacological activation of the ryanodine receptor in Jurkat T-lymphocytes. Br. J. Pharmacol. **128**, 1235–1240
31 Cancela, J. M., Churchill, G. C. and Galione, A. (1999) Coordination of agonist-induced Ca^{2+}-signalling patterns by NAADP in pancreatic acinar cells. Nature (London) **398**, 74–76
32 Berg, I., Potter, B. V. L., Mayr, G. W. and Guse, A. H. (2000) Nicotinic acid adenine dinucleotide phosphate (NAADP(+)) is an essential regulator of T-lymphocyte $Ca(^{2+})$-signaling. J. Cell. Biol. **150**, 581–588
33 Aarhus, R., Dickey, D. M., Graeff, R. M., Gee, K. R., Walseth, T. F. and Lee, H. C. (1996) Activation and inactivation of Ca2+ release by NAADP+. J. Biol. Chem. **271**, 8513–8516
34 Genazzani, A. A., Empson, R. R. and Galione, A. (1996) Unique inactivation properties of NAADP-sensitive Ca2+ release. J. Biol. Chem. **271**, 11599–11602
35 Navazio, L., Bewell, M. A., Siddiqua, A., Dickinson, G. D., Galione, A. and Sanders, D. (2000) Calcium release from the endoplasmic reticulum of higher plants elicited by the NADP metabolite nicotinic acid adenine dinucleotide phosphate. Proc. Natl. Acad. Sci. U.S.A. **97**, 8693–8698
36 Mojzisova, A., Kritanova, O., Zacikova, L., Kominkova, V. and Ondrias, K. (2001) Effect of nicotinic acid adenine dinucleotide phosphate on ryanodine calcium release channel in heart. Pflügers Arch. Eur. J. Physiol. **441**, 674–677
37 Bak, J., Billington, R. A., Timar, G., Dutton, A. C. and Genazzani, A. A. (2001) NAADP receptors are present and functional in the heart. Curr. Biol. **11**, 987–990
38 Copello, J. A., Qi, Y., Jeyakumar, L. H., Ogunbunmi, E. and Fleischer, S. (2001) Lack of effect of cADP-ribose and NAADP on the activity of skeletal muscle and heart ryanodine receptors. Cell Calcium **30**, 269–284
39 Higashida, H., Egorova, A., Higashida, C., Zhong, Z. G., Yokoyama, S., Noda, M. and Zhang, J. S. (1999) Sympathetic potentiation of cyclic ADP-ribose formation in rat cardiac myocytes. J. Biol. Chem. **274**, 33348–33354
40 De Toledo, F. G. S., Cheng, J., Liang, M., Chini, E. N. and Dousa, T. P. (2000) ADP-Ribosyl cyclase in rat vascular smooth muscle cells: properties and regulation. Circ. Res. **86**, 1153–1159

Received 12 April 2002/25 June 2002; accepted 9 July 2002
Published as BJ Immediate Publication 9 July 2002, DOI 10.1042/BJ20020584